Membrane topology of the *Escherichia coli* γ-aminobutyrate transporter: implications on the topography and mechanism of prokaryotic and eukaryotic transporters from the APC superfamily

Liaoyuan A. HU and Steven C. KING[1]

Department of Physiology and Biophysics, University of Texas Medical Branch, 301 University Blvd., Galveston, TX 77555-0641, U.S.A.

The *Escherichia coli* γ-aminobutyric acid permease (GabP) is a plasma membrane protein from the amine–polyamine–choline (APC) superfamily. On the basis of hydropathy analysis, transporters from this family are thought to contain 12, 13 or 14 transmembrane domains. We have experimentally analysed the topography of GabP by using the cytoplasmically active LacZ (β-galactosidase) and the periplasmically active PhoA (alkaline phosphatase) as complementary topological sensors. The enzymic activities of 32 GabP–LacZ hybrids and 43 GabP–PhoA hybrids provide mutually reinforcing lines of evidence that the *E. coli* GabP contains 12 transmembrane segments that traverse the membrane in a zig-zag fashion with both N- and C-termini facing the cytoplasm. Interestingly, the resulting model predicts that the functionally important 'consensus amphipathic region' (CAR) [Hu and King (1998) Biochem. J. **330**, 771–776] is at least partly membrane-embedded in many amino acid transporters from bacteria and fungi, in contrast with the apparent situation in mouse cationic amino acid transporters (MCATs), in which this kinetically significant region is thought to be fully cytoplasmic [Sophianopoulou and Diallinas (1995) FEMS Microbiol. Rev. **16**, 53–75]. To the extent that conserved domains serve similar functions, the resolution of this topological disparity stands to have family-wide implications on the mechanistic role of the CAR. The consensus transmembrane structure derived from this analysis of GabP provides a foundation for predicting the topological disposition of the CAR and other functionally important domains that are conserved throughout the APC transporter superfamily.

INTRODUCTION

The γ-aminobutyric acid permease (Gab; *gab* permease), an archetypal amine–polyamine–choline (APC) superfamily transporter [1], catalyses translocation of γ-aminobutyric acid (GABA) across the plasma membrane of Gram-negative [2–5] and Gram-positive [6] bacteria. Members of the APC superfamily are found broadly distributed in the plasma membranes of yeast, fungi and eubacteria, in which they function as transporters and/or retroviral receptors [7].

Recently a consensus amphipathic region (CAR) has been described to occur [2] in a multitude of transporters including numerous GabP homologues from the APC family, and in non-homologous GABA transporters from mammalian nervous system. The CAR is functionally significant in both the GabP [2], and the mammalian mouse cationic amino acid transporter (MCAT) proteins [8]. The channel-forming nature of the CAR suggests that it might be involved in the substrate translocation pathway [2], and elements within it (e.g. the GabP 'signature cysteines') are known to affect the rate of critical conformational changes associated with substrate translocation [9]. Interestingly, however, the topological disposition of the CAR is ambiguous. On the basis of hydropathy analysis [10], the CAR is believed to be membrane-embedded (appropriate for pore formation) in some proteins [2] and cytoplasmic (inappropriate for pore formation) in others [8].

In that conserved domains are expected to serve a similar function, learning whether the CAR [2,8] and other functionally important domains [11,12] are membrane-embedded or cytoplasmic will be a crucial element in understanding how they participate in transport catalysis. The topological analysis of GabP is significant because it provides an experimental foundation for predicting the topological disposition of functionally important domains in other transporters from the APC superfamily. In the absence of a three-dimensional structure, topological considerations necessarily serve as the main point of departure for experimental approaches aiming at resolving structure–function relationships.

EXPERIMENTAL

Materials

Enzymes for molecular biology were all from the New England Biolabs (Beverley, MA, U.S.A.). Sequenase® (version 2) DNA sequence kits were from Amersham Life Science (Arlington Heights, IL, U.S.A.). QIAprep Spin Miniprep kits from Qiagen (Chatsworth, CA, U.S.A.) were used to prepare plasmid DNA. Ultraclean® 15 kits (MoBio Labs, CA, U.S.A.) were used to purify DNA from agarose. Miller's Luria–Bertani (LB) medium was from Life Technologies (Gaithersburg, MD, U.S.A.). [^{3}H]-GABA (31.6 Ci/mmol) was from DuPont New England Nuclear (Boston, MA, U.S.A.). Cellulose acetate filters (0.45 μm) were from Micron Separations (Westboro, MA, U.S.A.). Liquiscint® scintillation cocktail was from National Diagnostics (Atlanta,

Abbreviations used: APC superfamily, amine–polyamine–choline transporter superfamily; CAR, consensus amphipathic region; GABA, γ-aminobutyric acid; GabP, γ-aminobutyric acid permease; IPTG, isopropyl β-D-thiogalactoside; LB, Luria–Bertani; MCAT, mouse cationic amino acid transporter; SPS, GabP 'sensitive polar surface' [Hu and King (1998) Biochem. J. **330**, 771–776]; TM, transmembrane segment; X-Gal, 5-bromo-4-chloroindol-3-yl β-D-galactopyranoside.

[1] To whom correspondence should be addressed (e-mail steven.king@utmb.edu).

Table 1 Plasmids and *E. coli* strains

Plasmids and strains	Relevant genotype and/or comments (chromosome/plasmid)	Source or reference
pSCK-380	$-/amp^r\ lacI^q\ tac\ O^+P^+$	[4]
pSCK-472B1	pSCK-380 derivative with BamH I site removed and with *gabP* gene in the *XhoI*/*NotI* sites	Present study
pSCK-380Z	pSCK-380 with *lacZ* insertion in *PstI*/*XhoI* sites	Present study
pSCK-380A	pSCK-380 with *phoA* insertion in *PstI*/*XhoI* sites	Present study
pSCK-GP7	pBluescript II KS(−) derivative carrying *gabP* gene	[4]
CC118	*ara*D139Δ(*ara leu*)7697 Δ*lac*X74 Δ*pho*A20 *gal*E*gal*K *thi rps*E *rpo*B *rec*A1/-	Dr. Colin Manoil [15]

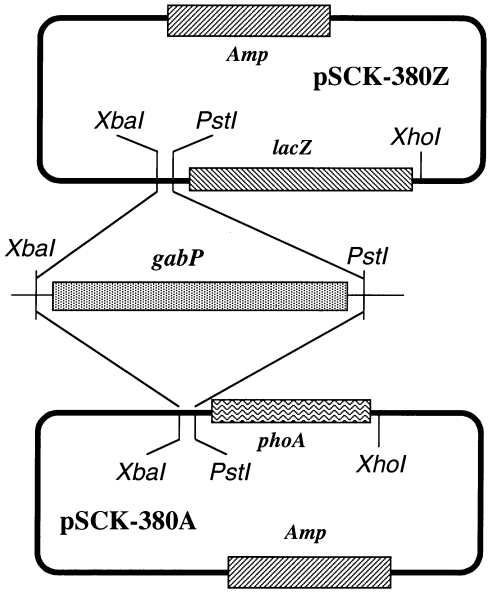

Figure 1 Structure of fusion vectors pSCK-380A and pSCK-380Z

The *gabP*, or its truncated derivatives produced by PCR, can be easily cloned into the *Xba*I/*Pst*I sites of either pSCK-380Z or pSCK-380A to produce in-frame *gabP–lacZ* or *gabP–phoA* gene fusions. The resulting fusion genes are under *lac* control so that fusion protein production is inducible by IPTG. A linker sequence, which is the same as that in the fusions obtained by the *in vivo* method, lies between the GabP fragment and the reporter enzyme as follows: GabP–AADSYTQVASWTEPFPFSIQGDP–reporter.

GA, U.S.A.). Isopropyl β-D-thiogalactoside (IPTG), *p*-nitrophenyl phosphate, *o*-nitrophenyl β-D-galactopyranoside, 5-bromo-4-chloroindol-3-yl β-D-galactopyranoside and all antibiotics were from Sigma (St. Louis, MO, U.S.A.). 5-Bromo-4-chloroindol-3-yl phosphate was from Boehringer Mannheim (Indianapolis, IN, U.S.A.). Other chemicals were from common commercial sources. The bacterial strains and plasmids used in this study are listed in Table 1. The plasmid pBlueScript II KS(−) was from Stratagene (La Jolla, CA, U.S.A.). The phages, λTn*lacZ*/in [13] and λTn*phoA* [14], were gifts from Dr. Colin Manoil (University of Washington, Seattle, WA, U.S.A.).

Plasmid construction

The fusion vectors pSCK-380Z and pSCK-380A (Figure 1), were constructed as described below. To construct pSCK-380Z, *lacZ* was amplified by PCR from the plasmid p472-G9Z (Fusion Z-1; see Table 2) by using the forward 'linker' primer 5′-GTC GCA ATT AGC GGT TTT TAC CCTGCAGAC TCT TAT ACA CAA GTA-3′ (*Pst*I site underlined), which anneals in the linker region of *gabP–lacZ* hybrids, and the reverse primer 5′-TGA TCT ACG CTCGAG TTA TTT TTG ACA CCA GAC-3′ (*Xho*I site underlined). The resulting PCR product, containing *lacZ*, was blunt-end ligated in the *Eco*RV site of the phagemid pBluescript II KS(−); the phagemid-borne *lacZ* was subcloned directionally in the *Pst*I/*Xho*I sites of the expression vector, pSCK-380, to create the plasmid pSCK-380Z (Figure 1).

To construct pSCK-380A, *phoA* was amplified from an *Escherichia coli mscL–phoA* fusion by using the forward 'linker' primer mentioned above, and a reverse primer, 5′-TGA TCT ACG CTCGAG TTA TTT CAG CCC CAG AGC G-3′ (*Xho*I site underlined). The N-terminal 537 bp of *gabP* was amplified by using the forward primer 5′-GCTCTAGAG AGA GGA TTC AGA TGG GGC AAT CAT CGC AA-3′ (*Xba*I site underlined) and reverse primer 5′-TAC TTG TGT ATA AGA GTCTGCAGG GTA AAA ACC GCT AAT TGC GAC-3′ (*Pst*I site underlined). Recombinant PCR was performed to join *gabP* and *phoA* at the common 'linker' region. The recombinant PCR product was purified from an agarose gel, then blunt-end ligated to the *Eco*RV site of the phagemid, pBluescript II KS(−). The *phoA* was excised from the phagemid, and then directionally subcloned into the *Pst*I/*Xho*I sites of pSCK-380 to create plasmid pSCK-380A (Figure 1).

Transposon-mediated fusions to *lacZ*

We followed the procedure described by Manoil [15] but with the use of λTn*lacZ*/in, an improved phage that provides a more efficient marker (i.e. sucrose sensitivity) for the selection of colonies with a plasmid-borne transposon insertion [13]. In brief, the cells (CC118) harbouring plasmid pSCK-472B1 were infected with λTn*lacZ*/in and the mixture was plated on LB agar supplemented with 100 μg/ml chloramphenicol to select cells with a transposon insertion. Plasmid DNA was isolated from the pool of chloramphenicol-resistant cells. The pooled plasmid was transformed into CC118 and selected on LB agar supplemented with 5% (w/v) sucrose, 40 μg/ml chloramphenicol, 0.4 mM IPTG, 80 μg/ml X-Gal and 100 μg/ml ampicillin. The blue, sucrose-resistant, kanamycin-sensitive colonies were those with a *lacZ* insertion but not the whole transposon. The exact insertion site was determined by sequencing across the *gabP–lacZ* junction by using the *lacZ* primer 5′-CGC CAG GGT TTT CCC AGT CAC GAC-3′.

Transposon-mediated fusion to *phoA*

A similar protocol was used for constructing the *gabP–phoA* fusion except that the λTn*phoA* phage (kanamycin-resistant) is used [15]. Gene fusions were selected on LB agar supplemented with 40 μg/ml kanamycin, 40 μg/ml 5-bromo-4-chloroindol-3-yl phosphate and 100 μg/ml ampicillin. The exact insertion site was

determined by sequencing across the *gabP–phoA* junction by using the *phoA* primer 5′-AAT ATC GCC CTG AGC A-3′.

Construction of GabP mutants with a 31-residue foreign epitope insertion

Plasmids encoding truncated GabP–LacZ hybrids were converted into constructs encoding 31-residue 'sandwich insertions' [13] by a simple procedure beginning with fusion constructs created with λTn*lacZ*/in. The fusion construct was digested to completion with *Bam*HI, and the largest of the resulting restriction fragments was recovered (UltraClean kit) after electrophoresis through 0.6% agarose. Finally the recovered fragment was treated with T4 DNA ligase. The resulting circular construct encoded a 'sandwich' featuring a 31-residue foreign peptide (inserted at the original fusion junction) flanked on each side by the wild-type GabP sequences. DNA sequencing was used to confirm that the *gabP* coding sequence was in frame with the sequence encoding the foreign epitope.

Transport activity

Overnight cells were diluted 1:100 into fresh LB medium containing 100 μg/ml ampicillin and 1 mM IPTG. Cells growing exponentially were harvested by centrifugation, washed twice with 100 mM phosphate buffer, pH 7.0, and finally resuspended in the same buffer such that the attenuance at 600 nm was between 6 and 7. Transport reactions were initiated by adding 90 μl of washed cells with rapid vortex-mixing to 10 μl of solution containing 100 μM [^{3}H]GABA (3 μCi/ml). Uptake was quenched by adding 1 ml of a 'stop solution' (buffer containing 20 mM $HgCl_2$) to the rapidly mixing reaction vessel. The 'quenched' sample was vacuum-filtered. The reaction vessel was then rinsed with 1 ml of 'wash buffer' (100 mM potassium phosphate, pH 7.0, containing 5 mM $HgCl_2$). Finally the filter was rinsed with 4 ml of 'wash buffer.' The washed filter was dissolved in scintillation cocktail and the radioactivity (d.p.m.) was calculated by a Beckman LS3801 scintillation spectrometer by using stored quenching curves and automatic quenching compensation (H number determination).

Site-directed gene fusion

A set of *gabP* truncations with fusion sites for *lacZ* (or *phoA*) were amplified from the pSCK-GP7 template by PCR. The forward primer, 5′-GCTCTAGAG AGA GGA TTC AGA TGG GGC AAT CAT CGC AA-3′ (*Xba*I site underlined), anneals to the 5′ end of *gabP* and introduces an *Xba*I site. The reverse primer anneals to *gabP* at the desired site for hybrid formation and introduces a *Pst*I site. The new restriction sites allow convenient cloning into the *Xba*I/*Pst*I site of the expression vector pSCK-380Z (to produce a GabP–LacZ hybrid) or pSCK-380A (to produce a GabP–PhoA hybrid) (Figure 1).

Enzymic activity of the fusions

The β-galactosidase activity was assayed as described by Miller [16]. In brief, the CC118 cells harbouring *gabP–lacZ* gene fusions were grown overnight and diluted 1:100 into fresh LB medium supplemented with 100 μg/ml ampicillin and 1 mM IPTG. The cells were grown to early exponential phase and placed on ice for 20 min before assay. The cells were permeabilized by adding two drops of 0.1% SDS and one drop of chloroform. The substrate *o*-nitrophenyl β-D-galactopyranoside was added, the mixture was incubated at 37 °C, and the reactions were quenched by the addition of 1 M Na_2CO_3. The enzyme activities are reported in Miller units [17]. Although expression levels can have a significant effect on the measured activity of enzymes [18], normalization to expression level or synthesis rate has little practical consequence and is not done [19,20] when complementary reporter enzymes are employed simultaneously to confirm topological assignments. The alkaline phosphatase activity was assayed by a similar procedure as described by Manoil [15], with *p*-nitrophenyl phosphate as substrate.

RESULTS

Construction of the gene fusions

An initial estimate of the GabP topology was obtained from hydropathy analysis (Figure 2), which is consistent with 12–14 transmembrane domains. To analyse in more detail the transmembrane topology of GabP, we used transposon-mediated gene fusions to construct many GabP–LacZ (Table 2) and GabP–PhoA (Table 3) hybrid proteins. Transposon insertion into the target gene was observed to be only quasi-random; 'hot spots' in *gabP* caused certain fusions to be isolated repeatedly (e.g. fusion Z-14, Z-23 and Z-26 in Table 2, and A-29 in Table 3), precluding efficient isolation of new fusion junctions. The PCR was used to avoid these 'hot spots' and to generate site-directed fusions. In total, 32 *gabP–lacZ* and 43 *gabP–phoA* fusions were constructed by the combined use of methods *in vivo* and *in vitro*. Importantly, this data set includes both a LacZ fusion and a PhoA fusion in every hydrophilic loop, providing complementary information to support the topological assignment of all loop domains (Tables 2 and 3).

Topological sensor activity

The dynamic range of alkaline phosphatase and β-galactosidase enzyme activities in the present study varied 100-fold. The clearest distinctions between high and low activities were obtained from GabP–LacZ fusions. The high-activity fusions (cytoplasmic) were typically over 1000 Miller units, whereas low activities were under 100 units (Figure 3, upper panel). GabP–PhoA fusions tended to exhibit a gradient of activities that were categorized as low (cytoplasmic), medium or high (Figure 3, lower panel). Thus the complementary enzymic activities of PhoA and LacZ were mutually reinforcing with only a single exception near the C-terminus of the first transmembrane domain (fusion Z-4). High activities were found for both β-galactosidase

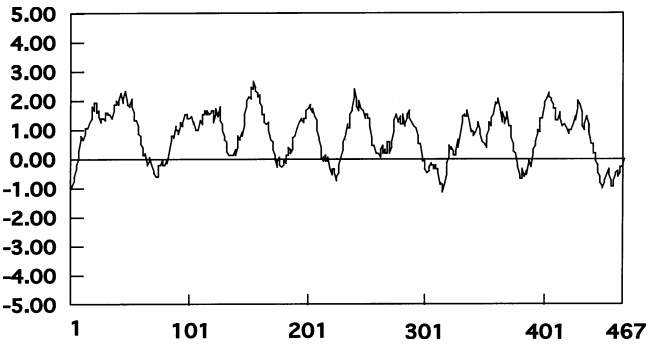

Figure 2 Hydropathy plot of the GABA transporter

Hydropathic indices were calculated with the method of Kyte and Doolittle [41], with a 20-residue window. Higher positive values represent greater hydrophobicity. This hydropathy plot indicates that GabP could contain at least 12 highly hydrophobic transmembrane domains flanked by hydrophilic domains.

Table 2 Locations and β-galactosidase activities of GabP–LacZ hybrid proteins

Fusion positions are named according to the last GabP amino acid residue before the reporter enzyme. Topological assignments are transmembrane domain (TM), cytoplasmic loop (C), periplasmic loop (P) and N- or C-terminus (NT or CT) as shown in Figure 4. Fusions constructed by PCR are marked by † and fusions retaining active GABA transport are marked by *.

Fusion no.	Position	Assignment	LacZ activity	Redundancy
Z-1	E9	NT	1715	1
Z-2	K15	NT	4832	1
Z-3	S31	TM1	2625	2
Z-4†	P45	P1	6783	–
Z-5†	A66	C1	3367	–
Z-6	G87	C1	1683	1
Z-7	W102	TM3	2183	1
Z-8†	S119	P2	156	–
Z-9	T134	TM4	63	1
Z-10	N141	TM4	54	1
Z-11†	E150	C2	4605	–
Z-12	Y178	P3	218	1
Z-13	E182	P3	58	1
Z-14	M196	P3	45	8
Z-15	G201	TM6	63	1
Z-16	V203	TM6	96	1
Z-17	M207	TM6	62	2
Z-18†	T221	C3	3640	–
Z-19†	A269	P4	30	–
Z-20	E278	P4	10	3
Z-21	I288	TM8	29	3
Z-22	A304	TM8	1747	1
Z-23	S316	C4	1805	16
Z-24	T333	C4	10727	4
Z-25†	A357	P4	86	–
Z-26	G368	TM10	68	10
Z-27	S381	TM10	71	1
Z-28†	A391	C5	6393	–
Z-29	Y403	TM11	5960	4
Z-30†	A426	P5	103	–
Z-31*†	P461	CT	2830	–
Z-32*†	P466	CT	2780	–

Table 3 Location and alkaline phosphatase activities of GabP–PhoA hybrid proteins

Fusion positions are named according to the last GabP amino acid residue before the reporter enzyme. Topological assignments are transmembrane domain (TM), cytoplasmic loop (C), periplasmic loop (P) and N- or C-terminus (NT or CT) as shown in Figure 4. Fusions constructed by PCR are marked by † and fusions retaining active GABA transport are marked by *.

Fusion no.	Position	Assignment	PhoA activity	Redundancy
A-1	K15	NT	9	2
A-2	S31	TM1	88	1
A-3	S37	TM1	3061	4
A-4†	P45	TM2	1568	–
A-5†	A66	C1	4	–
A-6	G91	TM3	58	1
A-7	G95	TM3	37	1
A-8†	A110	P2	1793	–
A-9	S119	P2	1658	–
A-10	T134	TM4	1298	1
A-11	L135	TM4	1258	1
A-12	S144	TM4	303	1
A-13†	E150	C2	5	–
A-14	A156	C2	495	5
A-15	I163	TM5	259	1
A-16	Y178	P3	2560	1
A-17†	P179	p3	1170	–
A-18	E182	P3	5748	1
A-19†	S187	P3	711	–
A-20	M196	P3	753	2
A-21	G201	TM6	3400	1
A-22†	T221	C3	181	–
A-23	A224	C3	181	–
A-24	N239	C3	1199	2
A-25†	A269	P4	1158	–
A-26	I293	TM8	2672	1
A-27	A304	TM8	247	1
A-28	R310	TM8	89	1
A-29	S316	C4	135	12
A-30	T333	C4	15	3
A-31	A355	TM9	9	1
A-32†	A357	P5	933	–
A-33	G368	TM10	3388	1
A-34	A371	TM10	1230	1
A-35†	A391	C5	0	–
A-36	L409	TM11	34	1
A-37	V417	TM11	2585	1
A-38†	A426	P6	1388	–
A-39	E430	TM12	3981	1
A-40	L437	TM12	2085	1
A-41	I442	TM12	1459	2
A-42	T444	TM12	473	2
A-43*†	P461	CT	5	–

and alkaline phosphatase at position 45, an observation inconsistent with the typical inverse relationship between these reporter enzymes. Anomalous high β-galactosidase activities are relatively common (observed in the mannose transporter [21], the Mtr permease [22] and the lysine permease [23]) in shorter fusion constructs involving the first periplasmic loop; they are considered to misrepresent the topology in this region [22,23]. In the present study, strict reliance on the LacZ activities to make topological assignments would lead to a model that placed the first 87 residues of GabP in the cytoplasm. This unlikely model is inconsistent with (1) the high PhoA activities measured at positions 37 and 45, and (2) with insertional mutagenesis studies (see below) that suggest that the secondary structure associated with transmembrane segment 1 (TM1) begins somewhere between residues 9 and 15.

Transport activity of N-terminal 'sandwich' insertions and C-terminal hybrids

Manoil and Bailey [13] have recently introduced the use of λTn*lacZ*/in as a tool for the construction of epitope tags that inactivate transport function when inserted into transmembrane segments. By using the well-understood and topologically characterized [24] *lac* permease as a model, these authors showed that loss of function was highly correlated with the insertion of epitopes into transmembrane domains rather than aqueous loops. Application of λTn*lacZ*/in to the *gab* permease (Table 4) suggests that an epitope positioned at Glu-9 lies innocuously in the cytoplasm (activity retained), whereas an epitope positioned at Lys-15 encroaches significantly (activity abolished) on the secondary structure leading into TM1. Similarly the GabP–LacZ hybrid formed at position 426 shows that truncation before TM12 abolishes function, whereas hybrids formed at distal positions in the cytoplasmic C-terminus [i.e. at positions 461 and 466 (the final residue)] have no effect on function.

DISCUSSION

Although topological information can be gleaned from several experimental approaches (chemical modification, limited pro-

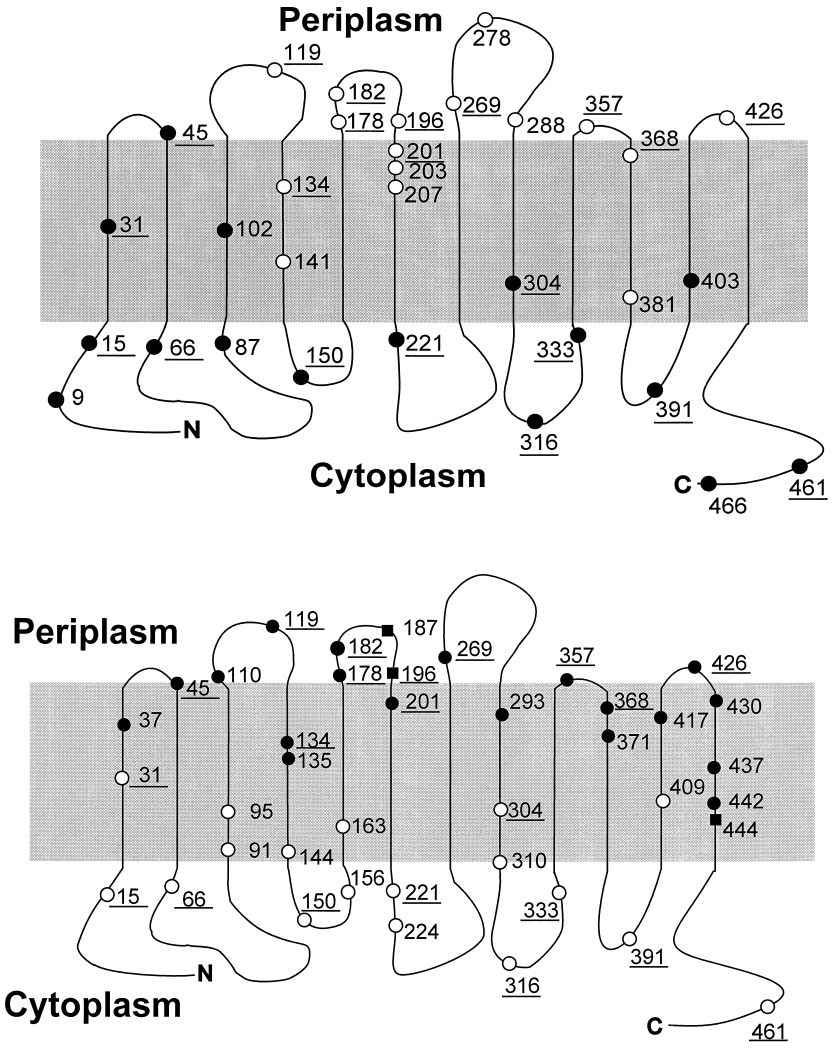

Figure 3 Application of GabP–reporter hybrid enzyme activities to the topology of GabP

The GabP polypeptide chain is shown crossing the membrane (grey area) 12 times in zig-zag fashion with the N- and C-termini retained in the cytoplasm. Experimentally determined reporter enzyme activities were applied to this putative structural arrangement with the position of GabP–LacZ or GabP–PhoA fusion junctions numbered from the last residue of the GabP sequence. Positions at which the topological assignment is confirmed with fusions to both LacZ and PhoA are underlined. In the upper panel low (less than 1000 units) and high (more than 1000 units) β-galactosidase activities are represented by ○ and ● respectively; in the lower panel, low (less than 500 units), intermediate (500–1000 units) and high (more than 1000 units) alkaline phosphatase activities are represented by ○, ■ and ● respectively. The units of activity for alkaline phosphatase and β-galactosidase were calculated as described previously [15,17].

Table 4 Transport activity of N-terminal and C-terminal mutations

A 31-residue 'sandwich' epitope insertion was placed at the indicated positions in the GabP N-terminal domain, and GabP–LacZ hybrids were formed at the indicated positions in the C-terminal domain. The ability of each construct to catalyse [^{3}H]GABA transport was assessed. Symbols: +, high transport activity; −, no transport activity. Abbreviation: n.a., results not available.

	Transport activity	
Junction	Epitope insertion	Hybrid
9	+	n.a.
15	−	n.a.
31	−	n.a.
426	n.a.	−
461	n.a.	+
466	n.a.	+

teolysis, immunochemical labelling [25,26]), we used the genetic approach developed by Manoil and Beckwith [27] to construct an extensive collection of GabP–LacZ and GabP–PhoA hybrid proteins in which LacZ and PhoA serve as topology sensors. In these hybrids the C-terminal portions of GabP are replaced by the topological reporter enzymes LacZ (β-galactosidase) and PhoA (alkaline phosphatase). Because these reporter enzymes lack intrinsic topogenic signals, their disposition across the membrane is determined solely by the topogenic signals arising from GabP. The transmembrane location of the fusion junction is thus reflected in the specific reporter enzyme activity exhibited by the GabP–LacZ or GabP–PhoA hybrid. The LacZ (native to the cytosol) is inactive if translocated to the outside, whereas alkaline phosphatase (native to the periplasm) is inactive when retained inside the cell. These two enzymes therefore function as complementary sensors that can provide important information on membrane protein topology [15].

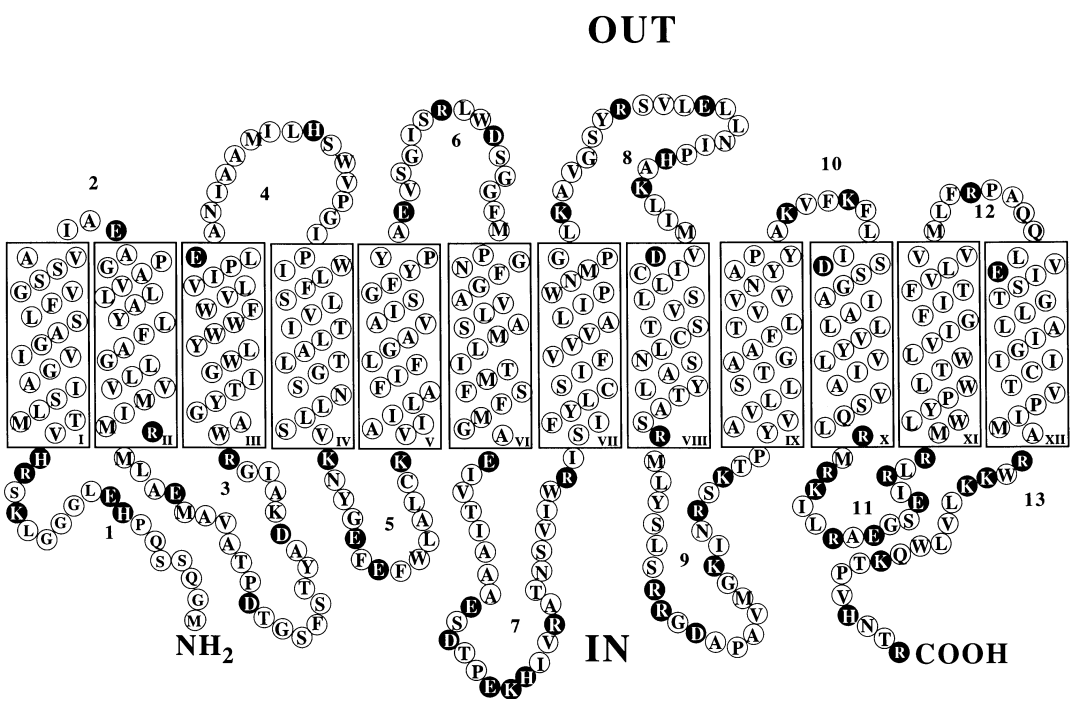

Figure 4 Proposed topological model of GABA transporter

This model has been drawn on the basis of multiple considerations: the hydropathy plot [41], the 'positive-inside' rule [28], the position of gaps in APC superfamily sequence alignments, and the experimental results obtained with GabP–LacZ and GabP–PhoA hybrids. The transmembrane domains (shown in boxes) contain 21 residues. The charged residues, indicated by filled circles, are almost completely excluded from the transmembrane domains. The model places several well-conserved charged residues in cytoplasmic loops 4–5 and 8–9. These conserved charges might be of broad functional significance in the APC superfamily [11,33].

In contrast, because hybrid proteins rarely retain transport activity, the extent of structural perturbation near the fusion junction cannot generally be ascertained. Thus, until confirmation from higher-resolution approaches has been obtained, it might be prudent to consider information from topological reporter enzymes as providing a reasonable, tentative, estimate of the actual topology, particularly with regard to the exact position of the transmembrane boundaries. Our estimate of the GabP topology derives from the following considerations.

Topological model of the GABA permease

On the basis of hydropathy analysis (Figure 2) and experimental results (Figure 3), we propose that the transmembrane topography of GabP includes 12 transmembrane domains that traverse the membrane in a zig-zag fashion, interconnected by hydrophilic loops (Figure 4). Both the N- and C-termini are placed in the cytosol, a conclusion strongly supported by several fusions (Z-1 and A-1 at the N-terminus; fusions Z-31, Z-32 and A-43 at the C-terminus). The distribution of the charged residues in this model is consistent with the 'positive-inside' rule [28]. Moreover, the model localizes the charged residues to loop regions and virtually excludes charges from the membrane (Figure 4). This organization of charge in GabP is different from the classical lactose permease in which several functionally important residues are membrane-embedded [29].

A consensus topology for the APC superfamily

GabP is homologous with many prokaryotic and eukaryotic transporters from the APC family [7,11]. These proteins all exhibit hydropathy profiles that suggest the presence of 12–14 transmembrane domains [30–32]. However, transporters that are from the same family and exhibit similar hydropathy profiles should have similar secondary structures and transmembrane topologies. Thus mapping the experimentally determined GabP topography on the predicated transmembrane domains in amino acid sequence alignments is expected to improve the predictive quality of the 'consensus' topological model for the APC superfamily (Figure 5).

In addition to the use of experimental results, two rules were also applied as constraints on the consensus model. First, an effort was made to minimize the number of charged residues buried in transmembrane domains. Secondly, gaps in the sequence alignment were relegated to loop regions on the theory that evolutionary 'insertions' into a secondary structure (i.e. a transmembrane helix) would be less tolerated than insertions into the connecting loops [19], a notion drawing support from recent studies on *lac* permease [13] and from the observation that APC transporters from eukaryotic cells are substantially larger than their prokaryotic homologues, the extra length seeming to have occurred within the more 'insertion-tolerant' hydrophilic loop regions.

Results of the analysis (Figure 5) show that there is overall agreement between (1) the 'consensus' topology defined here, (2) the topology predicted in the Swiss-Prot annotations (grey highlight) and (3) the experimentally confirmed topology of GabP (black highlight), especially in TMs 1, 2, 6, 7, 9, 10 and 11. Data from LysP [23], AroP [12] and PheP [33] also conform to this 'consensus' representation (Figure 5) of the APC family topology. In contrast, two transporters in Figure 5 (YikF and ProY) are predicted to contain 13 TMs. In that YikF and ProY

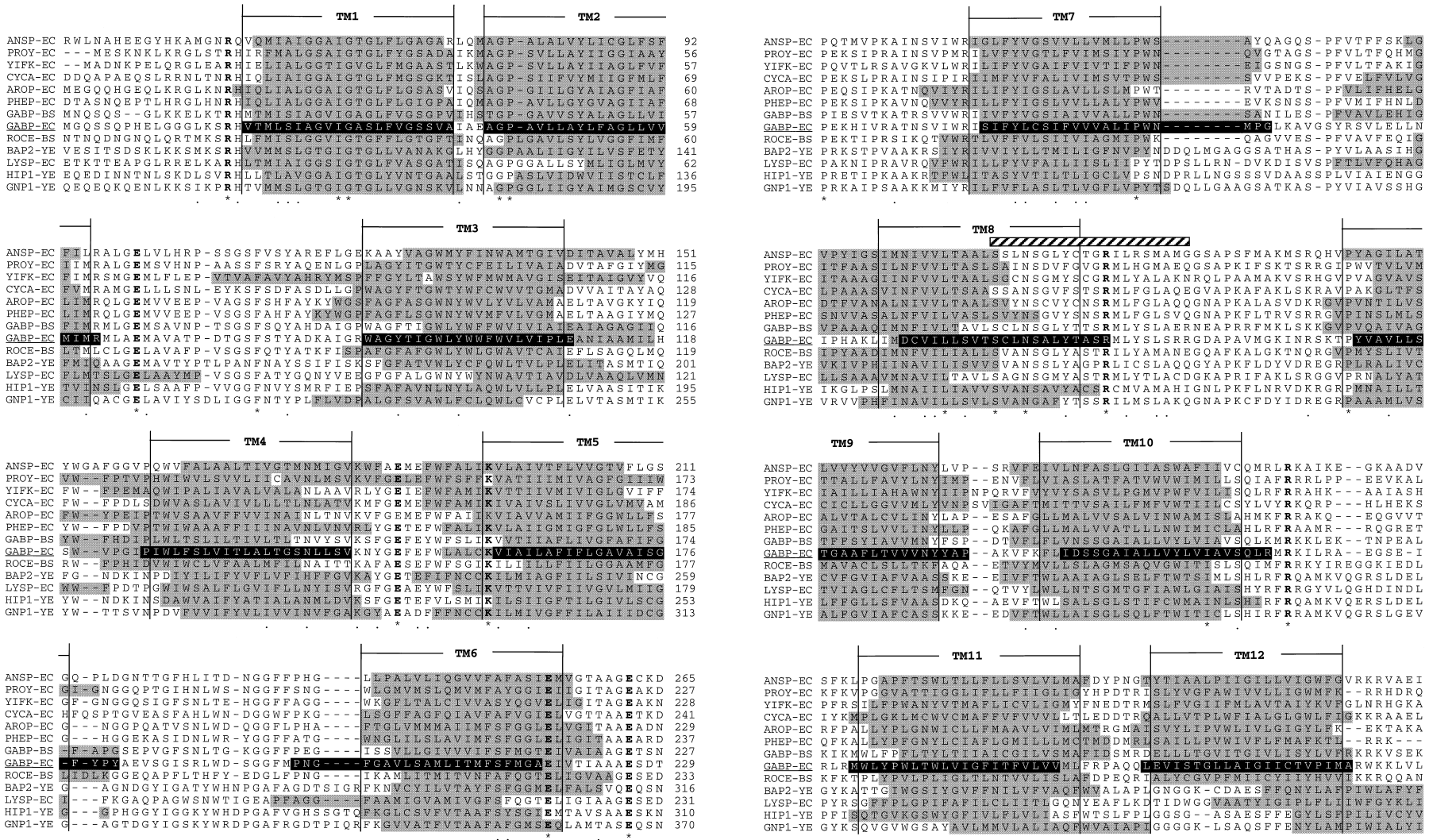

Figure 5 Multiple sequence alignment of the 13 transporters from APC superfamily

Amino acid sequences were excerpted from the Swiss-Prot database and aligned with program CLUSTAL W (1.5) [42] provided by the Bork group in the EMBL via the Internet (http://www.bork.embl-heidelberg.de/Alignment/). These transporters and their Swiss-Prot accession numbers are as follows: from *E. coli* (EC), L-asparagine permease (ANSP, p77610), proline-specific permease (PROY, p77327), D-serine/D-alanine/glycine transporter (CYCA, p39312), aromatic amino acid permease (AROP, p15933), phenylalanine-specific permease (PHEP, p24207), GABA permease (GABP, p25527), lysine-specific permease (LYSP, 25737) and putative amino acid permease (YIKF, p27837); from *Bacillus subtilis* (BS), GABA permease (GABP, p46349) and putative amino acid permeases (ROCE, p39137); from yeast (YE), Leu/Val/Ile permease (BAP2, p38084), histidine permease (HIP1, p06775) and glutamine permease (GNP1, p48813). The sequences shown are representative of over 30 homologous transporters (see the text) that could have been included; many were omitted from this alignment to save space. Asterisks mark residues conserved in all members, whereas dots mark positions occupied by highly similar residues; potential transmembrane domains (according to Swiss-Prot annotation) for each transporter are highlighted in grey; experimentally confirmed transmembrane domains of the *E. coli* GabP are highlighted in black; the 'consensus' transmembrane regions (TM) are marked by vertical lines. The GabP SPS is indicated by the hatched horizontal bar. Each consensus TM was set based on collective consideration of experiments, hydropathy and two rules applied by Buhr and Erni [19]: (1) minimize the number of charged residues within the transmembrane helix, and (2) where possible exclude from potential transmembrane domains any gaps in the amino acid sequence alignment.

are highly similar (from the same APC family subgroup) to GabP, these proteins should probably be represented by a 12-helix model.

Topology of functionally significant regions

The topological organizations of AroP and PheP are controversial in the region surrounding transmembrane domains 4 and 5. Whereas one model [33] maximizes the number of charges consigned to cytoplasmic loop 4–5 [as does the consensus model (Figure 5)], a recent study [12] favours minimizing the length of loop 4–5 to bury two highly conserved (and functionally important) glutamate residues within TM5. On the basis of the classical LacY paradigm, it might be expected that functionally important ionizable groups should be membrane-embedded [29]. In contrast, it is increasingly recognized that 'loop' regions can be important determinants of transport kinetics and ligand recognition properties, particularly in GABA transporters [2,34] and other proteins from the APC superfamily [8,35].

In transporters from the APC superfamily, helix 8 and the adjoining cytoplasmic loop 8–9 comprise a highly conserved CAR. Perturbation of residues on the polar face of a 20-residue 'window' (exactly the number needed to traverse a lipid bilayer) within the CAR is highly deleterious to GabP function [2] and defines the GabP 'sensitive polar surface' (SPS) (Figure 5). Because amphipathic segments [36,37] seem to be capable of making transient movements in and out of the membrane, the CAR could provide the basis for effecting a 'mobile barrier' mechanism of translocation catalysis [38]. In this regard, the present study is of interest because it provides a structural basis for understanding recent work on the susceptibility of the GabP 'signature cysteine' to attack by thiol-modifying reagents.

Whereas a GabP mutant containing a single cysteine residue at position 300 is readily inactivated by benzophenone maleimide (which partitions strongly into lipid and fails to react with aqueous thiols [39]), exhaustive treatment with [2-(trimethylammonium)ethyl]methanethiosulphonate or 2-sulphonatoethylmethanethiosulphonate (which are membrane-impermeable thiol reagents that bear fixed charges [40]) fails to cause inactivation (L. A. Hu and S. C. King, unpublished work). Although transmembrane domain boundaries cannot in general be defined with great precision, these chemical modification studies are nevertheless well explained by the present results, which have relied on topological reporter enzymes to infer that 'signature cysteine' [9] lies within TM8 so that the GabP SPS seems to extend out of the membrane and into the cytoplasmic space. This topological disposition is distinct from (1) TM8 assignments made on the basis of multiple sequence alignments (Figure 5, grey areas) or (2) the presumed situation in the MCAT proteins, in which the homologous region is thought to be contained entirely within the loop connecting TMs 8 and 9 [8,35].

Although additional work is needed to resolve the topological ambiguity of the CAR completely in different proteins, an understanding that the GabP SPS is at least partly membrane-embedded provides a basis for understanding how this potential channel-forming domain might function family-wide.

Received 8 June 1998/12 August 1998; accepted 11 September 1998

This work was supported by a grant-in-aid from the American Heart Association, Texas Affiliate, Inc.

REFERENCES

1 Niegemann, E., Schulz, A. and Bartsch, K. (1993) Arch. Microbiol. **160**, 454–460
2 Hu, L. A. and King, S. C. (1998) Biochem. J. **330**, 771–776
3 King, S. C., Fleming, S. R. and Brechtel, C. E. (1995) J. Biol. Chem. **270**, 19893–19897
4 King, S. C., Fleming, S. R. and Brechtel, C. E. (1995) J. Bacteriol. **177**, 5381–5382
5 Brechtel, C. E., Hu, L. and King, S. C. (1996) J. Biol. Chem. **271**, 783–788
6 Brechtel, C. and King, S. C. (1998) Biochem. J. **333**, 565–571
7 Reizer, J., Finley, K., Kakuda, D., MacLeod, C. L., Reizer, A. and Saier, Jr., M. H. (1993) Protein Sci. **2**, 20–30
8 Closs, E. I., Lyons, C. R., Kelly, C. and Cunningham, J. M. (1993) J. Biol. Chem. **268**, 20796–20800
9 Hu, L. A. and King, S. C. (1998) J. Biol. Chem. **273**, 20162–20167
10 Sophianopoulou, V. and Diallinas, G. (1995) FEMS Microbiol. Rev. **16**, 53–75
11 Pi, J., Wookey, P. J. and Pittard, A. J. (1993) J. Bacteriol. **175**, 7500–7504
12 Cosgriff, A. J. and Pittard, A. J. (1997) J. Bacteriol. **179**, 3317–3323
13 Manoil, C. and Bailey, J. (1997) J. Mol. Biol. **267**, 250–263
14 Manoil, C. and Beckwith, J. (1985) Proc. Natl. Acad. Sci. U.S.A. **82**, 8129–8133
15 Manoil, C. (1991) Methods Cell Biol. **34**, 61–75
16 Miller, J. H. (1972) in Experiments in Molecular Genetics, pp. 398–404, Cold Spring Harbor Laboratory, Cold Spring Harbor, NY
17 Miller, J. H. (1972) in Experiments in Molecular Genetics, pp. 352–355, Cold Spring Harbor Laboratory, Cold Spring Harbor, NY
18 San Millan, J. L., Boyd, D., Dalbey, R., Wickner, W. and Beckwith, J. (1989) J. Bacteriol. **171**, 5536–5541
19 Buhr, A. and Erni, B. (1993) J. Biol. Chem. **268**, 11599–11603
20 Jording, D. and Pühler, A. (1993) Mol. Gen. Genet. **241**, 106–114
21 Huber, F. and Erni, B. (1996) Eur. J. Biochem. **239**, 810–817
22 Sarsero, J. P. and Pittard, A. J. (1995) J. Bacteriol. **177**, 297–306
23 Ellis, J., Carlin, A., Steffes, C., Wu, J., Liu, J. and Rosen, B. P. (1995) Microbiology **141**, 1927–1935
24 Calamia, J. and Manoil, C. (1990) Proc. Natl. Acad. Sci. U.S.A. **87**, 4937–4941
25 Traxler, B., Boyd, D. and Beckwith, J. (1993) J. Membr. Biol. **132**, 1–11
26 Jennings, M. L. (1989) Annu. Rev. Biochem. **58**, 999–1027
27 Manoil, C. and Beckwith, J. (1986) Science **233**, 1403–1408
28 von Heijne, G. (1992) J. Mol. Biol. **225**, 487–494
29 Kaback, H. R. (1996) in Handbook of Biological Physics, vol. 2 (Konings, W. N., Kaback, H. R. and Lolkema, J. S., eds.), pp. 203–227, Elsevier, Amsterdam
30 Weber, E., Chevallier, M. R. and Jund, R. (1988) J. Mol. Evol. **27**, 341–350
31 Vandenbol, M., Jauniaux, J. C. and Grenson, M. (1989) Gene **83**, 153–159
32 Henderson, P. J. F. (1993) Curr. Opin. Cell Biol. **5**, 708–721
33 Pi, J. and Pittard, A. J. (1996) J. Bacteriol. **178**, 2650–2655
34 Tamura, S., Nelson, H., Tamura, A. and Nelson, N. (1995) J. Biol. Chem. **270**, 28712–28715
35 Closs, E. I., Graf, P., Habermeier, A., Cunningham, J. M. and Forstermann, U. (1997) Biochemistry **36**, 6462–6468
36 Slatin, S. L., Qiu, X.-Q., Jakes, K. S. and Finkelstein, A. (1994) Nature (London) **371**, 158–161
37 Qiu, X. Q., Jakes, K. S., Finkelstein, A. and Slatin, S. L. (1994) J. Biol. Chem. **269**, 7483–7488
38 Henderson, P. J. F. (1991) Biosci. Rep. **11**, 477–535
39 Jones, P. C., Sivaprasadarao, A., Wray, D. and Findlay, J. B. C. (1996) Mol. Membr. Biol. **13**, 53–60
40 Holmgren, M., Liu, Y. and Yellen, G. (1996) Neuropharmacology **35**, 797–804
41 Kyte, J. and Doolittle, R. F. (1982) J. Mol. Biol. **157**, 105–132
42 Higgins, D. G., Thompson, J. D. and Gibson, T. J. (1996) Methods Enzymol. **266**, 383–402